Available online at www.sciencedirect.com
SCIENCE DIRECT®
Dyes and Pigments 71 (2006) 218–223
DYES and PIGMENTS
www.elsevier.com/locate/dyepig

An NMR and UV–visible spectroscopic study of the principal colored component of *Stil de grain* lake

A. Romani*, C. Zuccaccia, C. Clementi

Dipartimento di Chimica, Università di Perugia, Via Elce di Sotto 8, 06123 Perugia, Italy

Received 24 June 2005; accepted 7 July 2005
Available online 19 September 2005

Abstract

Water extract from rhamnus berries (*Rhamnus catharticus*) is the base of Stil de grain lake (also called Buckthorn lake), an ancient dye used in textiles and in paintings. In this work, the main colored component of the lake was separated and its chemical structure determined by advanced NMR techniques. The results show that quercitrin, a glucoside derivative of quercetine (3,5,7,3′,4′-pentahydroxy-flavone) is the principal colored form. This result does not agree with previous literature assignments. In this work a characterization of quercitrin in methanol and in water as a function of pH was carried out by absorption and emission UV–visible spectroscopy.

Keywords: Stil de grain lake; Ancient dye; Luminescence properties; NMR advanced techniques

1. Introduction

From the 14th to 19th centuries, lake pigments were essential constituents of the artist's palette [1]. These translucent pigments were obtained by precipitating or adsorbing an organic dye onto an inert inorganic substrate. Stil de Grain, also called Rhamno lake or Spincervino lake or Buckthorn lake, is one of these lakes; the gold-yellow dye which constitutes this lake is obtained by extraction with hot water from the berries of *Rhamnus catharticus*, a wild plant diffused in the northern hemisphere, in Brazil and southern Africa. Rhamnus dye is known since ancient time and was largely used, as a lake, from middle age to XIXth century for dying textiles. Other artistic techniques like miniature, tempera and oil employed this lake during the same period [2]. The main colorant present in the water extract from rhamnus berries is reported to be a glycoside derivative of rhamnetin (3,5,3′,4′-tetrahydroxy-7-methoxy-flavone) [2–5].

Identification of materials, principally organic, used in artworks by non-destructive techniques is not an easily achievable goal and many researchers involved in the restoration and conservation fields have been investigating the suitability of almost all the known spectroscopic techniques. Absorption and emission UV–visible spectroscopy has been suggested as a method for identifying organic dyes [6,7], pigments and binders [8] used in paint. Knowledge of the chemical composition of materials constituting an artistic object is essential in order to understand the mechanism of degradation: studying the medium acidity effects on the photophysical properties of dyes is a way for understanding chromatic modifications [9] and photo-aging processes [10].

In this work, the main component of the water extract from rhamnus berries was isolated by HPLC and identified by NMR as quercitrin (2-*O*-quercetil-5-*O*-β-pyranosyl-L-rhamnoside) [11], a glucoside derivative of quercetine (3,5,7,3′,4′-pentahydroxy-flavone), different

* Corresponding author. Tel.: +39 075 585 5620; fax: +39 075 585 5598.
E-mail address: romani@unipg.it (A. Romani).

0143-7208/$ - see front matter © 2005 Elsevier Ltd. All rights reserved.
doi:10.1016/j.dyepig.2005.07.005

from that assigned in the literature. Absorption and luminescence properties of this compound in methanol and in water, as a function of pH, were also investigated.

2. Materials and methods

Rhamno berries were purchased from Kremer (Farbmühle, Germany). Methanol for spectroscopic investigations was a Fluka spectrograde product used without further purification. To determine the pK values, Britton buffers prepared with re-distilled water were used in the 2–12 pH range. For chromatographic separation methanol and water BDH, HPLC solvents, and tri-fluoro acetic acid (TFA) Aldrich were used. Waters 600 HPLC Chromatograph with Waters 996 Photodiode Array detector and Waters Xterra MS C_{18} 5 μm analytic and semi-preparative columns were used for chromatographic separation. In both analytical and preparative HPLC, gradient elution was used. For analytical purposes the ratio of ethanol/water (0.1% TFA) was 10/90 v/v during the first 10 min and then varied with a linear gradient up to 100/0 in 60 min. In the preparative method, the methanol/water (0.1% TFA) ratio was 18/82 v/v for the first 3 min and then varied up to 100/0 in 35 min.

Absorption spectra in solution were recorded with a Perkin Elmer Lambda 800 spectrophotometer. Corrected emission spectra were obtained using a Spex fluorolog-2 FL 112 spectrofluorimeter controlled by Spex Datamax spectroscopy software. The emission quantum yield was obtained by comparing corrected areas of the sample and the standard (quinine sulfate in 1 N H_2SO_4, $\Phi_{ST} = 0.546$) [12] emission, using Eq. (1) which accounts for the differences in absorbance and refraction index of the sample (A_S, n_s) and the standard (A_{ST}, n_{ST}) solutions.

$$\Phi_F = \Phi_{ST} \frac{A_{ST} \times \text{area}_S \times n_S^2}{A_S \times \text{area}_{ST} \times n_{ST}^2} \quad (1)$$

The emission lifetime (τ_F) was determined by using the Pockels cell of the Spex spectrofluorimeter accessory based on the phase-shift method (time resolution: 30 ps). The light scattered by an aqueous glycogen solution (undetectable fluorescence) was used as a standard. The accuracy of the data obtained depended on the emission intensity.

Low ionic strength Britton buffers ($\mu = 0.01$ mol dm^{-3}) were used to determine the pK values. The pH values were measured with an Orion 9103 pH-meter. Sample concentrations were of the order of 10^{-5} mol dm^{-3}. Given the low concentration and low ionic strength of the solutions, the activity coefficient ratio of the acid–base couples was considered to be one.

Deuterated methanol from Cortec was used, without further purification, for NMR analysis. NMR spectra were recorded on a Bruker Avance DRX 400 spectrometer equipped with QNP probe with z-gradient coil. Gradient pulses were generated by using the GREAT 1/10 gradient unit. Sample temperature was controlled using the BVT 3000 variable temperature unit equipped with digital control. All the spectra were processed using XwinNMR 3.2 Bruker software.

^{1}H, ^{13}C{^{1}H}, ^{13}C ATP (attached proton test), ^{1}H COSY (COrrelation SpectroscopY), ^{1}H NOESY (Nuclear Overhauser Effect SpectroscopY), ^{1}H, ^{13}C HMQC (Heteronuclear Multiple Quantum Coherence), and ^{1}H, ^{13}C HMBC (Heteronuclear Multiple Bond Correlation) [13] spectra were recorded in CD_3OD at 298 K. Sample temperature was measured using a 4% CH_3OH in CD_3OD standard tube. Spectra are reported in δ scale (ppm) downfield with respect to TMS and referenced to the residual solvent signals (3.31 ppm for ^{1}H and 49.0 ppm for ^{13}C). Coupling constants (J) are given in Hertz; the following abbreviations are used: s = singlet, d = doublet, dd = doublet of doublet, ddd = doublet of doublet of doublet, t = triplet, q = quartet, m = multiplet. NMR data for *2-O-quercetil-5-O-β-pyranosyl-*L*-rhamnoside (quercitrin)*: (see Scheme 1 for numeration) ^{1}H NMR: $\delta = 7.34$ (d, $^4J_{HH} = 2.1$, H5), 7.30 (dd, $^3J_{HH} = 8.3$, $^4J_{HH} = 2.1$, H3), 6.90 (d, $^3J_{HH} = 8.3$, H2), 6.39 (d,

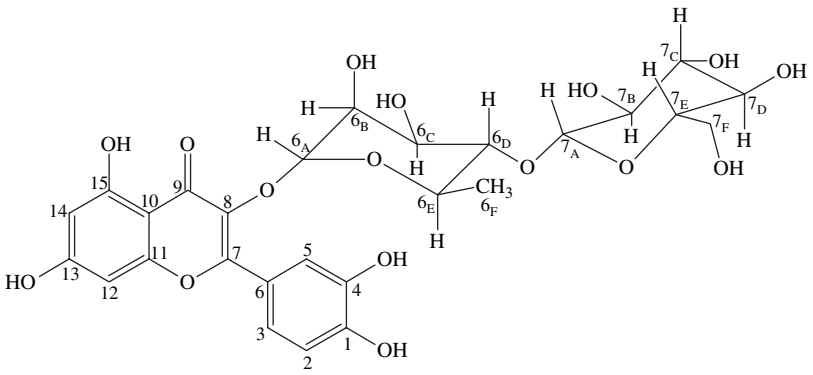

Scheme 1.

$^4J_{HH}$ = 2.1, H12), 6.21 (d, $^4J_{HH}$ = 2.1, H14), 5.39 (d, $^3J_{HH}$ = 1.7, $H6_A$), 4.50 (d, $^3J_{HH}$ = 7.9, $H7_A$), 4.24 (dd, $^3J_{HH}$ = 3.3, $^3J_{HH}$ = 1.7, $H6_B$), 3.98 (dd, $^3J_{HH}$ = 9.4, $^3J_{HH}$ = 3.3, $H6_C$), 3.81 (dd, $^2J_{HH}$ = 11.9, $^3J_{HH}$ = 2.1, $H7_{F'}$), 3.66 (dd, $^2J_{HH}$ = 11.9, $^3J_{HH}$ = 5.0, $H7_{F''}$), 3.54 (*pseudo* t, $^3J_{HH}$ = 9.5, $H6_D$), 3.41 (dd, $^3J_{HH}$ = 9.5, $^3J_{HH}$ = 6.2, $H6_E$), 3.37 (*pseudo* t, $^3J_{HH}$ = 8.7, $H7_C$), 3.31 (m, $H7_D$, buried under residual solvent signal), 3.25 (ddd, $^3J_{HH}$ = 9.1, $^3J_{HH}$ = 5.0, $^3J_{HH}$ = 2.2, $H7_E$), 3.19 (dd, $^3J_{HH}$ = 9.0, $^3J_{HH}$ = 7.9, $H7_B$) 1.01 (d, $^3J_{HH}$ = 6.2, $H6_F$). $^{13}C\{^1H\}$ *NMR*: δ = 179.6 (s, C=O), 165.9 (s, C13), 163.2 (s, C15), 159.4 (s, C7), 158.5 (s, C11), 149.8 (s, C1), 146.4 (s, C4), 135.9 (s, C8), 122.9 (s, C6), 122.7 (s, C3), 117.0 (s, C5), 116.4 (s, C2), 105.9 (s, C10), 105.3 (s, $C7_A$), 103.0 (s, $C6_A$), 99.8 (s, C14), 94.7 (s, C12), 82.8 (s, $C6_D$), 78.2 (s, $C7_C$), 77.9 (s, $C7_E$), 75.9 (s, $C7_B$), 72.0 (s, $C6_C$), 71.7 (s, $C6_B$), 71.4 (s, $C7_D$), 70.5 (s, $C6_E$), 62.6 (s, CH_2), 17.9 (s, $C6_F$).

3. Results and discussion

3.1. Separation and identification of quercitrin

Rhamno berries were ground in a mortar and the paste obtained was extracted with boiling water, as reported in an ancient recipe for the lake preparation [2]. The solution obtained was analyzed by HPLC. The chromatogram is shown in Fig. 1.

The compound corresponding to the main colored specie was isolated and its structure, shown in Scheme 1, was determined by NMR. (Numbering of C atoms in the flavone moiety is not that conventionally used but represent the NMR assignment.)

The ^{1}H NMR spectrum consists of 18 signals, only one of these integrating for three protons, while there are 27 resonances in the ^{13}C NMR spectrum. ^{13}C ATP NMR experiment revealed that 11 resonances are due to quaternary or secondary carbons, while the remaining 16 resonances correspond to primary or tertiary carbon

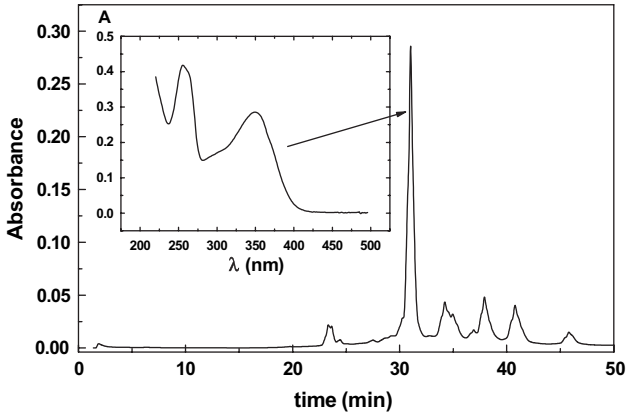

Fig. 1. HPLC chromatogram of the water extract from rhamno berries. Inset: absorption spectrum corresponding to the main peak (quercitrin).

atoms. The peak assignment starts from the observation that of the 11 ^{13}C resonances corresponding to quaternary or secondary carbons, only the one at 62.6 ppm shows heteronuclear single-bond correlation (^{1}H, ^{13}C HMQC spectrum) with the two proton resonances at 3.81 and 3.66 ppm; these resonances are assigned to $C7_F$, $H7_{F'}$ and $H7_{F''}$, respectively. Starting from $H7_{F'}$ and $H7_{F''}$, and following scalar interactions (^{1}H COSY, Fig. 2), proton resonances $H7_A$–$H7_E$ can be straightforwardly assigned; ^3J coupling constant values and dipolar interaction of $H7_A$ with both $H7_E$ and $H7_C$ in the ^{1}H NOESY spectrum are consistent with the proposed glucopyranosyl structure of the 7_A–7_F ring. Observation of a strong ^{1}H NOESY cross peak between $H7_A$ and the signal at 3.54 ppm allowed proton $H6_D$ to be identified (Fig. 3A); as before, ^3J coupling constant values, ^{1}H COSY (Fig. 2) and ^{1}H NOESY were used for the assignment of the stereochemistry of protons $H6_A$–$H6_C$, $H6_E$ and $H6_F$, which is consistent with the proposed rhamnopyranosil structure of the 6_A–6_F ring. With proton assignment in hand, the corresponding carbon resonances of the diglucoside moiety can be straightforwardly recognized from the ^{1}H, ^{13}C HMQC spectrum. Two pieces of experimental evidence support the connection between the disaccharide fragment and the chromophore to be at C8 position. First, a long-range scalar interaction (^{1}H, ^{13}C HMBC spectrum, Fig. 4) is observed between $H6_A$ and the carbon resonance at 135.9 ppm; lack of other multiple bond C–H correlations for this resonance is in agreement

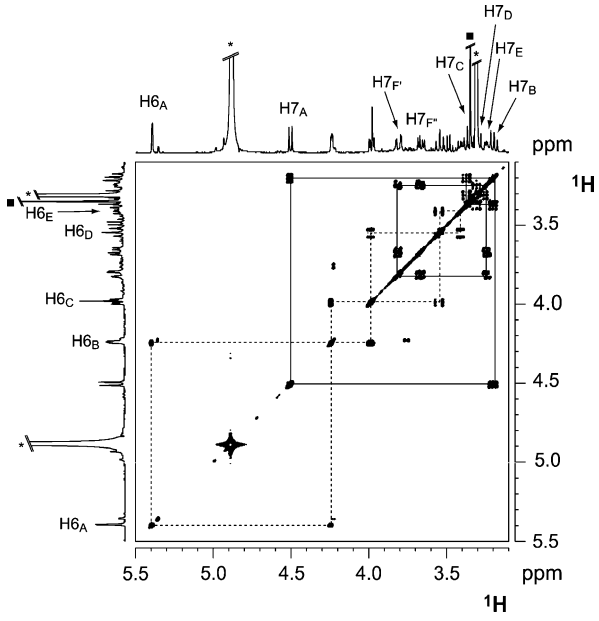

Fig. 2. Section of the ^{1}H COSY spectrum of the main product obtained by HPLC separation (CD_3OD, 298 K). Scalar connectivities inside the 6_A–6_F and 7_A–7_F pyranosil rings are evidenced. For the sake of clarity, the $H6_E$–$H6_F$ connection is not included in this section. Symbols * and ■ mark signals due to CD_2HOH and CH_3OH, respectively.

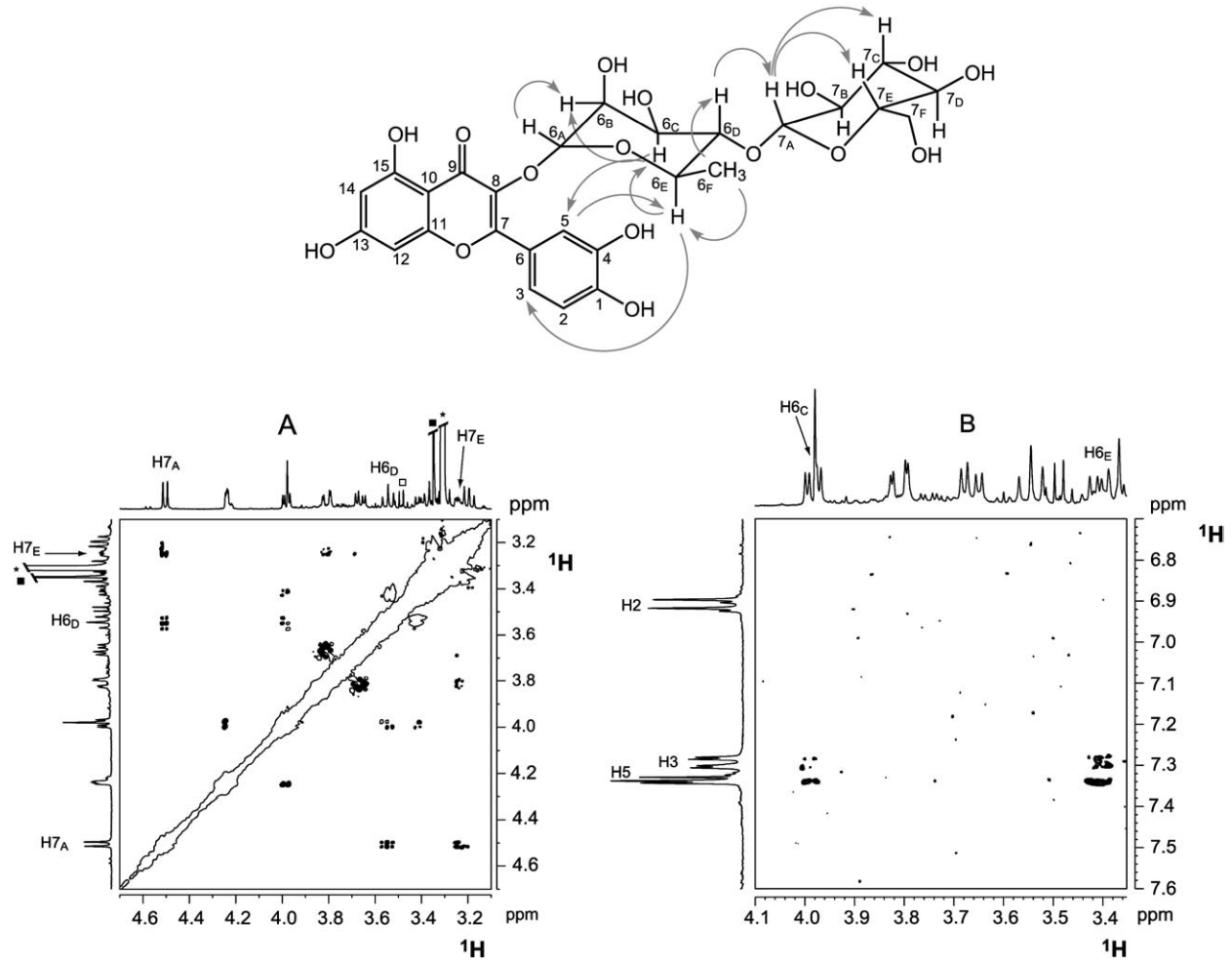

Fig. 3. Two sections of the ^{1}H NOESY spectrum of the main product obtained by HPLC separation (CD_3OD, 298 K, $\tau_m = 800$ ms), showing (A) the dipolar interaction between $H6_D$ and $H7_A$, and (B) the cross peaks between $H6_C$ and $H6_E$ with both H5 and H3. Arrows in the molecular sketch indicate relevant NOE interactions not included in these sections. Symbols ∗ and ■ mark signals due to CD_2HOH and CH_3OH, respectively.

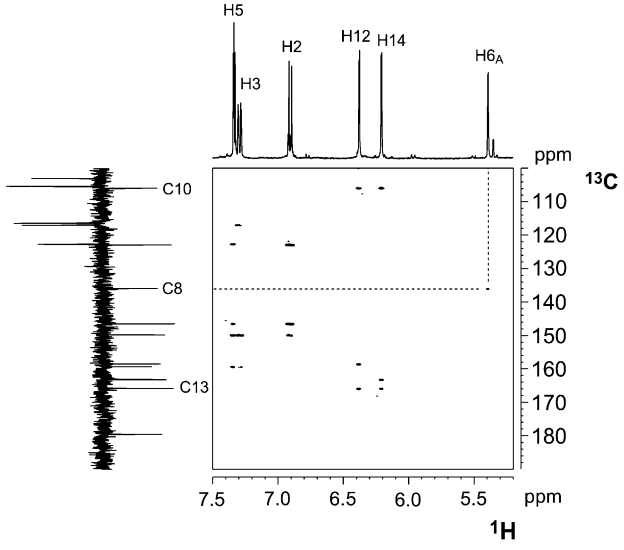

Fig. 4. Section of the ^{1}H, ^{13}C HMBC spectrum of the main product obtained by HPLC separation (CD_3OD, 298 K), showing, in particular, the long-range correlation between $H6_A$ and C8.

with its assignment to C8. Second, weak, but detectable, ^{1}H NOESY cross peaks are present between $H6_E$ and $H6_C$ with the two aromatic signal at 7.34 and 7.30 ppm (Fig. 3B) that are assigned to H5 and H3, respectively. Proton and carbon resonances of the C1–C6 phenyl ring are finally recognized by crossing the information coming from ^{1}H COSY, ^{1}H, ^{13}C HMQC and ^{13}C HMBC experiments, while ^{1}H, ^{13}C HMBC spectrum allows C7 resonance at 159.4 to be identified. Spectral pattern of the remaining aromatic ^{1}H resonances at 6.39 and 6.21 ppm are consistent with a phenyl ring having two CH groups in *meta* relative position. Two additional evidences support the positioning of this CH groups in 12 and 14 positions; first, there are two carbon resonances at 165.9 and 105.9 ppm showing similar long-range correlation with both H12 and H14; second, the carbon resonance at 179.6 ppm that falls in the expected region of carbonyl groups, does not show any long-range scalar interactions with any proton resonances. Unambiguous assignment of H12 and H14 as well as C10–C15 is achieved by simulation (ACD/NMR

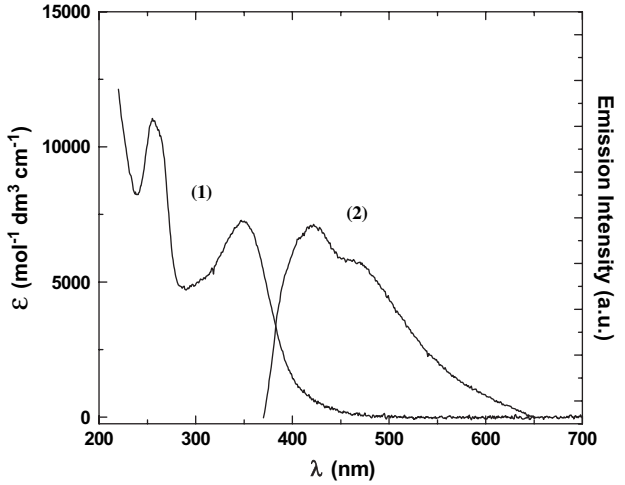

Fig. 5. Absorption (1) and emission (2) spectra of quercitrin in methanol.

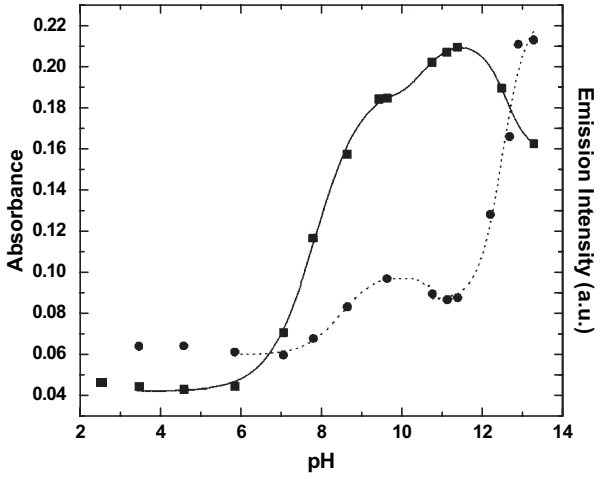

Fig. 6. Spectrophotometric (squares, monitored at 386 nm) and fluorimetric (circles, monitored at 460 nm) titration curves for quercitrin.

Predictor software by Advanced Chemistry Development Inc.) of proton and carbon spectra of the proposed aromatic fragment in which the glucoside moiety has been replaced by an OCH_3 group.

3.2. Spectral characterization

Absorption and emission spectra of quercitrin in methanol are shown in Fig. 5. The absorption spectrum ($\lambda_{max} = 256$ and 350 nm) is characteristic of flavonoids and the emission spectrum ($\lambda_{max} = 425$ nm) is attributed to quercitrin, also based on the good overlap of the absorption and emission excitation spectra. The emission from quercitrin is assigned as fluorescence on the basis of its location, its spectral distribution which mirrors the absorption and its measured lifetime. Due to the low emission quantum yield (2×10^{-4}) the measured lifetime of 0.7 ns has a large uncertainty.

3.3. Acid–base properties

Four distinct species were detected from both the absorption and emission (quercitrin shows fluorescence over the whole pH range) spectral changes in the pH range explored (pH 2–12). In Table 1, absorption and emission maxima, Stokes shift and frequency of the 0–0 transition are shown. The Stokes shifts, determined from the energy difference between the lowest energy absorption and the highest energy emission maxima of each species, decrease as the negative charge of the anions increases. This indicates a decrease in the stabilization energy of the excited state when the negative charge increases.

In Fig. 6, absorbance and fluorescence signals at constant wavelength are plotted as a function of the pH. Both trends show similar inflection points, indicating that fluorescence emission is faster than acid–base equilibration in the excited state [14], as previously found for similar molecules [9]. The estimated pKs, which are reported in Table 2, are affected by great uncertainties, due to proximity of the pHs at which the equilibrations occur. The excited state pKs*, calculated using the thermodynamic Föster cycle [15], are also reported. The frequency differences between 0 and 0 levels, needed to calculate the pK^*, were obtained from the intersections of the normalized absorption and emission spectra. The significant increase in acidity of the neutral form in the excited state ($\Delta pK \sim 5$) is in accord with results obtained for similar molecules [9,10,16]. A tentative proposal for the deprotonation steps is shown in Scheme 2.

The first deprotonation is localized on the 7-OH which is the most acidic site. The following acid–base equilibration involves the 3′- or 4′-OH, due to their long distance from the negative charge. 5-OH is probably the

Table 1
Absorption and emission spectral properties of quercitrin as a function of pH

pH	Absorption λ_{max} (nm)	Fluorescence λ_{max} (nm)	ν_{0-0} (cm^{-1})	$\Delta\nu$ (cm^{-1}) Stoke-shift
3.21 (neutral)	343	437	26 670	6270
9.21 (monoanion)	379	459	24 270	4600
10.25 (dianion)	383	457	24 040	4230
12.70 (trianion)	386	417	24 940	1920

Table 2
Dissociation constants of quercitrin in the ground and excited states and relative variation

	pK	ΔpK^*	pK^*
pK_1	7.5	−4.9	2.6
pK_2	10	−0.5	9.5
pK_3	>12	+1.8	>13.8

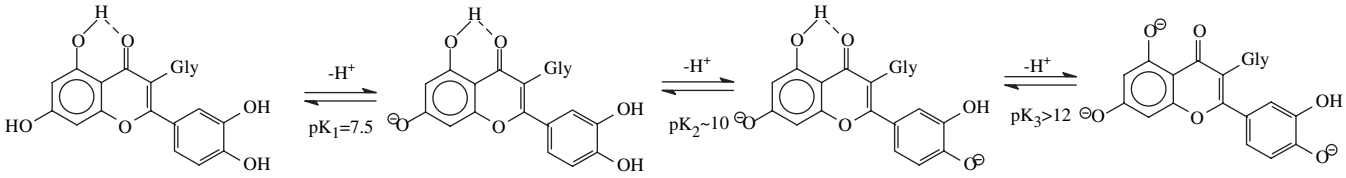

Scheme 2.

last one due to its partial hydrogen-bond with the carbonyl group.

4. Conclusions

The results of this work show how advanced NMR techniques, such as ^{1}H NOESY, ^{1}H COSY, ^{1}H, ^{13}C HMQC and ^{1}H, ^{13}C HMBC, are powerful tools for identifying the complex chemical structure of naturally occurring dyes. The spectral properties, here determined for quercitrin, are diagnostic means for identifying the dye present in an artwork, especially as they can be used in a portable set-up for in situ non-invasive measurements.

The study of the pH effect on absorption and emission spectra allowed the ground and excited state p*K*s to be estimated. Four different forms, stable in certain pH intervals, were spectrally characterized. This provides a valuable analytical tool for investigating interactions involving hydrogen transfer processes between the dye and its chemical environment.

Acknowledgements

The research was funded by the Ministero per l'Università e la Ricerca Scientifica e Tecnologica (Rome) and the University of Perugia in the framework of the Programmi di Ricerca di Interesse Nazionale.

References

[1] Saunders D, Kirby J. Light-induced colour changes in red and yellow lake pigments. Natl Gallery Techn Bull 1994;15:79.
[2] La fabbrica dei colori. Roma: Bagatto Libri; 1995. p. 230–2.
[3] <http://www.ibiblio.org/herbmed/eclectic/kings/rhamnus-cath.html>.
[4] <http://www.npicenter.com/library/herbal/materiamedica/HAWTHORN.asp>.
[5] Martuscelli E. I coloranti naturali nella tintura della lana: Collana di trasferimento e diffusione, vol. 2. Roma: Edizioni Campec; 2003. p. 69.
[6] Billmeyer Jr FW, Kumar R, Saltzman M. Identification of organic colorants in art objects by solution spectrophotometry. J Chem Educ 1981;58:307–13.
[7] Miliani C, Romani A, Favaro G. A spectrophotometric and fluorimetric study of some anthraquinoid and indigoid colourants used in artistic paintings. Spectrochim Acta Part A 1998;54:581–8.
[8] Renè de la Rie E. Fluorescence of paint and varnish layers (Part I). Stud Conserv 1982;27:1–7;
Renè de la Rie E. Fluorescence of paint and varnish layers (Part II). Stud Conserv 1982;27:65–9;
Renè de la Rie E. Fluorescence of paint and varnish layers (Part III). Stud Conserv 1982;27:102–8.
[9] Miliani C, Romani A, Favaro G. Acidichromic effects in 1,2- and 1,2,4-hydroxyanthraquinones. A spectrophotometric and fluorimetric study. J Phys Org Chem 2000;13:141–50.
[10] Favaro G, Miliani C, Romani A, Vagnini M. Role of protolytic interactions in photo-aging processes of the red lake pigment in solution and painted layers. J Chem Soc Perkin Trans 2 2002;192–7.
[11] <http://39.1911encyclopedia.org/G/GL/GLUCOSIDE.Htm>.
[12] Meech SR, Phillips D. Photophysics of some common fluorescence standards. J Photochem 1983;23:193–217.
[13] Sanders JKM, Hunter BK. Modern NMR spectroscopy. 2nd ed. New York: Oxford University Press; 1993.
[14] Ireland JF, Wyatt PAH. Acid–base properties of electronically excited states of organic molecules. Adv Phys Org Chem 1976;12:131–221.
[15] Förster T. Influence of pH on the fluorescence of naphthalene derivatives. Z Electrochem 1950;54:531–5.
[16] Richtol HH, Fitch BR. Excited singlet state acidity constants for hydroxy and amino substituted anthraquinones and related compounds. Comparison of excited-state p*K* measurement procedures. Anal Chem 1974;46:1749–54.